Available online at www.sciencedirect.com
SCIENCE DIRECT®
ELSEVIER
Organic Geochemistry 37 (2006) 280–290
Organic Geochemistry
www.elsevier.com/locate/orggeochem

Characteristics and origin of natural gases in the Kuqa Depression of Tarim Basin, NW China

Yan-Rong Zou [a,*], Changyi Zhao [b], Yunpeng Wang [a], Wenzhi Zhao [b], Ping'an Peng [a], Yanhua Shuai [a,b]

[a] The State Key Laboratory of Organic Geochemistry, Guangzhou Institute of Geochemistry, Chinese Academy of Sciences, Wushan, P.O Box 1131, Guangzhou, Guangdong 510640, China
[b] The Research Institute of Petroleum Exploration and Development, PetroChina, Beijing 100083, China

Received 25 July 2005; accepted 2 November 2005
(returned to author for revision 24 October 2005)
Available online 10 January 2006

Abstract

Significant gas condensate as well as some black oils have been discovered in the Kuqa Depression of Tarim Basin, NW China. Dry gases with high $\delta^{13}C$ values occur in the Kelasu structural belt, wet, isotopically light gases in the Yiqikelik belt, whereas condensates are distributed mainly in the Front Uplift area. Kinetic modeling results show that the variation of methane and ethane isotopes with increasing vitrinite reflectance is independent of heating rates for a given source rock. Two maturity trends have been observed on a C_2/C_1–$\delta^{13}C_1$ plot, one for thermogenic gases associated with coal, another for oil-associated gases with minor contribution from biogenic gas. It is most likely that the gases in the Kelasu belt and Front Uplift area were derived from the Jurassic coal measures and Triassic lacustrine shales, respectively, with those in the Yiqikelik belt being the mixtures of gases from the two sources. Both Jurassic coals and Triassic lacustrine shales appear to have contributed to the gases in the Kela 2 (KL2) and Dina 2 (DN2), the two largest gas fields in the Tarim Basin.

1. Introduction

The origin of natural gas is closely related to the diagenetic and thermal alteration of organic matter (Schoell, 1980, 1983). It is widely accepted that most of the natural gases accumulated in the subsurface reservoir are generated from thermal degradation of sedimentary organic matter. Natural gas is dominated by a few simple, low-molecular weight gaseous hydrocarbons. Important genetic information is commonly obtained from stable carbon and hydrogen isotope compositions. Stable isotope measurements on natural gases provide a kind of "fingerprint" used to assess the nature and thermal maturity of potential source rock, the pathway of gas migration, the presence of mixed-source gases and, more controversially, reservoir accumulation/loss histories (Tang et al., 2000). The stable carbon isotope compositions of individual light hydrocarbon components are the most important parameters to classify natural gases with respect to their generation processes and post-genetic histories (Cramer et al.,

* Corresponding author. Tel.: +8620 8529 0187; fax: +8620 8529 0706.
E-mail address: zouyr@gig.ac.cn (Y.-R. Zou).

0146-6380/$ - see front matter
doi:10.1016/j.orggeochem.2005.11.002

2001). Stable carbon isotopic and chemical compositions of natural gases have been used to identify both the type of their source organic matter (Schoell, 1980, 1983; Mattavelli et al., 1983; Faber and Stahl, 1984), and the maturity of source rocks (Stahl and Carey, 1975; Stahl, 1977; Schoell, 1983; Clayton, 1991).

In past years, a few isotope kinetic models have been developed to describe and predict the variation in the $\delta^{13}C$ compositions of methane during natural gas generation (Galimov, 1988; Cramer et al., 1998, 2001; Tang et al., 2000). Several gas compositional and isotopic cross-plots are employed to distinguish source and maturity related changes in natural gases from those caused by post-generation processes (Prinzhofer and Huc, 1995; Prinzhofer and Pernaton, 1997; Lorent et al., 1998; Prinzhofer et al., 2000). This manuscript presents the results of a case study of natural gases in the Kuqa Depression of Tarim Basin, NW China, with a focus on the gas compositional and isotopic variations as a function of their source rock maturity.

2. Geological setting

The Kuqa Depression, bounded to the north by the South Tianshan Mountains, is a secondary structural unit within the northern Tarim Basin (Fig. 1). This depression contains significant gas condensate resources, as well as small amounts of black oil (Fig. 1). Several giant gas fields, including the KL2 and DN2, have been discovered in Cretaceous and Tertiary reservoirs.

The Kuqa Depression consists of three structural belts, i.e., the Kelasu–Yiqikelik in the north; the Qiulitak in the middle, and the Front Uplift in the south. The Kelasu–Yiqikelik belt bears mostly gas pools, the Qiulitak belt both oil and gas pools, with the Front Uplift belt being characterized by gas condensate pools with some black oil (Fig. 1). The maturity level of the Lower Jurassic rocks in the deepest parts of the Kuqa Depression may have reached up to 3.0 %Ro (Liang et al., 2002, 2003).

Available data (Lin et al., 2002; Li et al., 2003) indicate that the Kuqa Depression was filled with Late Permian to Quaternary terrestrial clastic rocks. The potential hydrocarbon source rocks in this depression are the Upper Triassic lacustrine shales/mudstones and thin coal beds formed in fluvio-deltaic and lacustrine systems, and the Lower-Middle Jurassic coal beds deposited in a swamp-lacustrine environment. The Jurassic coal-bearing sequence consists of thick mudstones intercalated with sandstone bodies and thick coal seams (Zhang et al., 2002a,b; Liu et al., 2003a,b). The sandstone bodies provide excellent pore spaces for natural gas migration and entrapment. The type III organic-rich Jurassic source rocks are mainly distributed in the Kelasu-Yiqikelik belt, whereas the type II Triassic lacustrine source rocks extend to the northern portion of this belt (Liang et al., 2003).

Wang et al. (1999, 2000) reconstructed the burial and thermal histories of the Kuqa Depression. During the Mesozoic this depression appeared to have a low sedimentation rate, with about 4000 m of sediments being deposited by the end of the Cretaceous (over about 180 Ma). The geothermal gradients during the Mesozoic period were also low, probably in the range of 29–32 °C/km. During the Cenozoic,

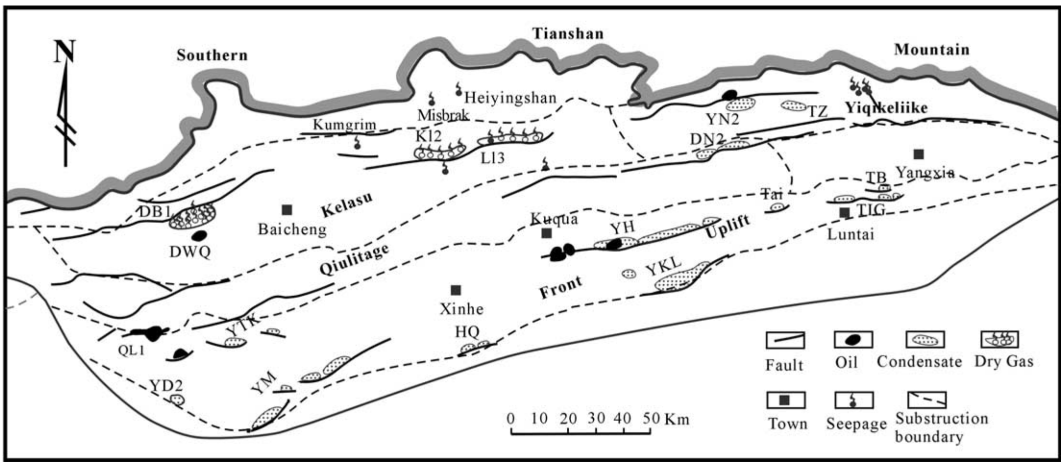

Fig. 1. Structural subdivisions and gas field distribution in the Kuqa Depression of the Tarim Basin.

especially in the Neogene, over 4700 m of Neogene red beds were deposited near the depocenter (Baicheng area, Fig. 1), with the geothermal gradients being around 29 °C/km. This was followed by the deposition of 2500 m of N_2–Q sediments over the last 5 Ma. The current geothermal gradient in the Kuqa Depression is around 25 °C/km. The lowest vitrinite reflectance values of the Jurassic coals observed from the surrounding outcrops are all higher than 0.80 %Ro, near the peak of oil generation.

A close association between the fault system and oil/gas field distribution is shown in Fig. 1, suggesting that faults have played important roles for the hydrocarbon migration and accumulation in this depression. According to Pi et al. (2002) and Song et al. (2002), this depression had been in continuous subsidence since the early Jurassic, except during a brief period of mild uplift at the end of the Cretaceous. There was an increase in compressional stress in this region from about 5.3–2.0 Ma. This was followed by the formation of thrust faults in the past 2 Ma, which cut through the source rocks into the bottom of the seals (Liu et al., 2001) and led to overpressure in many of the hydrocarbon pools (Pi et al., 2002; Song et al., 2002).

3. Samples and experimental conditions

3.1. Sample

As the maturity levels of all possible source rocks in the Kuqa Depression are over 0.80 %Ro, these rocks are not ideal candidates for laboratory pyrolysis experiments for simulating natural maturation processes. A low rank coal collected from the HYC1 well near the Kuqa Depression was selected in this study. This sample, sampled at the depth of 3334 m, shows a vitrinite reflectance value at 0.41 %Ro. Its basic geochemical characteristics are listed in Table 1, together with several other coal samples from the YN2 well and Kuqa Depression for comparison. The HYC1 sample was studied extensively previously (Liu et al., 2003a,b).

3.2. Experimental procedure

Anhydrous and hydrous pyrolysis in open or closed systems are commonly used to simulate petroleum generation in the subsurface. An open-system pyrolysis experiment is closely related to the primary cracking reactions of organic matter. Hydrous pyrolysis is the other simulation method for petroleum generation. As hydrous pyrolysis is limited by the maximum pyrolysis temperature due to excessive water and its critical point, the complete reaction of gas generation cannot be reached at the end of pyrolysis. Because of the strong adsorption capability, the early generated products (heavy hydrocarbon) will be prevented from expulsion from the coal sample and undergo secondary cracking into gas. Therefore, a dry, closed system pyrolysis is employed in this study to simulate gas generation from coal.

The coal sample was first ground into powder to 100 mesh (150 μm) after removing any potential contaminant from the core surface. Kerogen was isolated from the powdered sample using HCl/HF digestion (Durand and Nicais, 1980). Kerogen powder, 20–50 mg depending on the final temperature, was put into gold tubes and welded under an argon atmosphere after the complete removal of air. Then, the 15 welded tubes were placed in 15 autoclaves and heated in one single oven at heating rates of 2 and 20 °C/h. A pressure of 65 MPa was maintained during the pyrolysis experiment. At the end of the heating experiment, the autoclaves were rapidly cooled to ambient temperature in a water bath. The cleaned gold tubes were put in a vacuum system and pierced. The gas products were released from gold tubes and collected using a Toepler pump. The compositional analysis was performed on line with an HP5880A gas chromatograph. The external standard method was used to quantify the gas com-

Table 1
Basic geochemical data of the coal sample used in this study

Well	Depth (m)	Ro (%)	TOC (%)	T_{max} (°C)	S1 + S2 (mg/g)	HI (mgHC/gTOC)	δCorg (‰)
HYC1	3334	0.41	66.67	420	182.55	238	−24.20
YN2[a]	4310.23	0.90	76.50	448	119.14	215	−23.90
Kuqa[b] depression	∼>9000	0.8–3.0	(54.34)	440–570	46–197 (138)	150–280 (245)	−22.00 to −26.00

The number in parentheses indicates the arithmetic mean value.
[a] After Zhang et al. (2002a,b).
[b] After Li et al. (2004).

ponents. Details of both the pyrolysis system and vacuum system have described by Behar et al. (1992).

The stable carbon isotope composition of individual gaseous hydrocarbons was analyzed using a VG Isochrom II instrument equipped with a Poraplot Q column (30 m × 0.32 mm i.d. with 0.25 μm film thickness). A temperature program of 50 °C (2 min) to 180 °C (10 min isothermal) at 25 °C/min was used. A CO_2 gas is employed as reference gas to calibrate the isotope ratios of the samples measured. A standard mixture of gaseous hydrocarbons (C_1–C_4) calibrated with known isotopic composition was used to check the performance of the IRMS instrument. The precision of the instrument analysis is better than 0.3‰ for IRMS. The carbon isotopic compositions are reported in per mil (‰) relative to the PDB standard.

4. Results

4.1. Generation and carbon isotope compositions of methane and ethane

Both the chemistry and the isotopic signatures of the gaseous hydrocarbon provide the information of gas genesis and evolution (Prinzhofer et al., 2000). The chemical compositions and carbon isotope values of gaseous hydrocarbons are analyzed with GC and GC-IRMS, respectively. The chemical compositions and carbon isotope values of cumulative methane and ethane are presented in Table 2.

As shown in Table 2, methane is the predominant hydrocarbon component of the gases generated from coal. This is followed by ethane and C_3–C_5 alkanes, though in substantially reduced abundances. This study focuses on the kinetic modeling of the stable carbon isotope compositions of methane and ethane within increasing pyrolysis temperatures, and attempts to extrapolate the results into geological conditions.

4.2. Kinetics modeling

Natural gas generation, like the formation of oil from kerogen (Ungerer and Pelet, 1987; Schaefer et al., 1990; Schaefer et al., 1999), can be adequately described by a set of parallel, first-order reactions with a distribution of activation energies (E) and a single frequency factor (A). A commercial software package KINETICS2000 developed by Braun and Burnham (Lawrence Livermore National Laboratory, 1999) was used to obtain the kinetics parameters of natural gas, methane and ethane generation through fitting pyrolysis data at the two heating rates. A Gaussian distribution of activation energy is employed here to model gaseous hydrocarbon generation, including methane, ethane and total gas, because the activation-energy distribution is more rigorously correct and clearly relates to observed variations in product composition and because the shape of the reaction profile for petroleum source rocks was closely matched by the Gaussian distribution (Burnham and Braun, 1999).

The kinetics parameters of total gas (C_1–C_5 hydrocarbons) generation are shown in Fig. 2a, in which the Gaussian distribution of activation energy with a single frequency factor $A = 3.86 \times 10^{10}\ s^{-1}$

Table 2
The cumulative yields and stable carbon isotope compositions of methane and ethane generated from the pyrolysis of HYC1 coal

Pyrolysis at heating rate of 2 °C/h					Pyrolysis at heating rate of 20 °C/h				
T (°C)	Yield (ml/g TOC)		Isotope values (‰)		T (°C)	Yield (ml/g TOC)		Isotope values (‰)	
	Methane	Ethane	Methane	Ethane		Methane	Ethane	Methane	Ethane
318	0.92		−32.42		320	0.31		−29.40	
344	2.23	0.58	−33.83	−28.01	340	0.58	0.06	−30.90	
363	5.20	1.81	−34.90	−27.81	360	1.23	0.23	−32.70	
383	11.24	3.94	−36.08	−27.08	381	2.57	0.72	−33.87	−26.91
404	24.50	7.48	−36.5	−26.17	401	6.60	2.23	−34.77	−27.20
429	50.08	11.24	−35.25	−24.25	422	13.38	4.47	−35.50	−27.39
445	76.05	12.80	−33.83	−22.85	443	24.04	7.01	−35.86	−27.21
465	97.21	9.78	−31.75	−19.63	464	39.27	9.33	−35.59	−26.94
486	122.15		−29.50		484	60.23	10.36	−34.05	−26.31
506	140.21		−27.92		505	67.05	10.63	−32.85	−25.41
532	178.19		−26.50		531	100.44		−30.54	
557	184.00		−25.75		557	134.01		−27.48	
					580	146.99		−26.22	

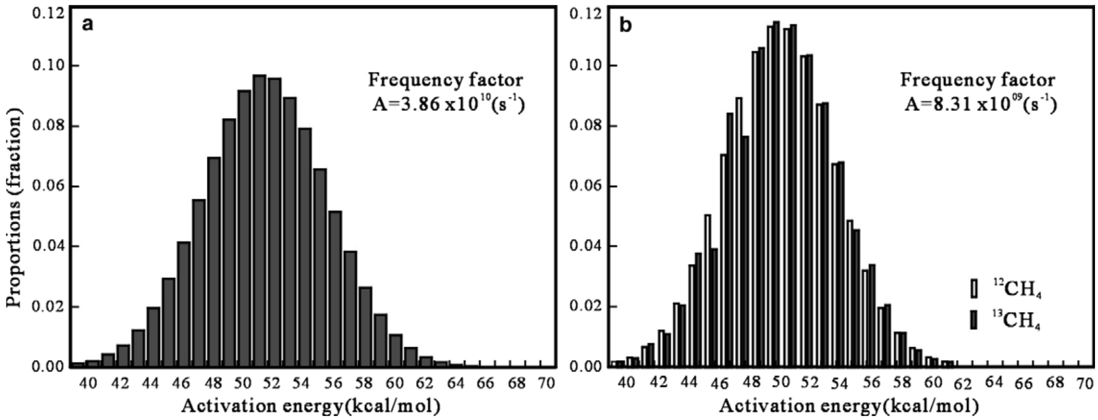

Fig. 2. The kinetic parameters of gaseous hydrocarbon generation (a) and methane carbon isotope modeling (b) derived from the pyrolysis of HYC1 coal.

has been determined. The parameters will be used to model the total gas generation under geological conditions.

The stable carbon isotope composition modeling of both methane and ethane is carried out, based on their generation kinetics. The isotopically light species is modeled with a Gaussian distribution activation-energy and a single frequency factor, while the isotopically heavy species is done with a distribution near to the Gaussian activation-energy. The frequency factor ratio of isotopically light/heavy species varies within a range of 1.02–1.04 (Tang et al., 2000), with 1.02 used here.

Carbon isotope compositions are frequently reported as δ-values, which are defined as

$$\delta^{13}\mathrm{C} = (R/\mathrm{Rstd} - 1) \cdot 1000(\mathrm{PDB}, ‰), \qquad (1)$$

where R denotes the $^{13}C/^{12}C$ ratio of product and Rstd the $^{13}C/^{12}C$ ratio of the PDB standard.

As is well known, the generated methane/ethane includes both ^{12}C- and ^{13}C-methane/ethane, but ^{12}C-bearing methane/ethane is predominant. Therefore, the kinetic parameters (i.e., frequency factor and activation-energy) of the total methane/ethane are taken as those of ^{12}C-bearing methane/ethane during isotope modeling. Thus, the kinetic parameters (frequency factor and activation-energy) of ^{12}C-bearing methane/ethane and the frequency factor ($A_{13} = 1.02 \cdot A_{12}$) of ^{13}C-bearing methane/ethane are known, another parameter of ^{13}C-bearing methane/ethane, activation-energy distribution, can be obtained by means of fitting the isotope values measured at different temperatures and heating rates. When these parameters are satisfactory to fit the generation and isotope data measured, the parameters can be applied to the geological conditions to model the variance in the isotope compositions of methane and ethane during the period of the geological history.

A spreadsheet program, EasyDelta, was employed when the isotope kinetics modeling was performed. The details of this spreadsheet program and the calculation procedure was described elsewhere (Zou et al., 2005). The activation-energy distributions of both $^{12}CH_4$ and $^{13}CH_4$ with a frequency factor of $^{12}CH_4$ generation are shown in Fig. 2b, the kinetics parameters of ethane are not shown.

As stated above, strong compressive stress occurred in the Kuqa Depression at around 5.3–2 Ma, with faults likely acting as important pathways for oil and gas migration. When faults cut through sandstone bodies, the gases migrated into the traps probably through the fault. Before this occurred, the gases in the sandstone bodies may have undergone secondary cracking, as indicated by the relatively high $\delta^{13}C$ values of C_{2+} gaseous hydrocarbons. Therefore, ethane cracking was also included in the ethane isotope modeling. The isotope modeling method used here for the ethane cracking is almost the same as for simulating its generation except for the replacement of the conversion of the ethane generation by the ethane cracking during the modeling. The point at which the ethane conversion is equal to 1.0 and the steady ethane isotope values are reached signals the end point of ethane generation and the starting point of ethane cracking. Whether the ethane cracking occurs depends strongly on the thermal history a gas underwent.

The vitrinite reflectance is computed with the kinetics parameters of Easy%Ro (Sweeney, 1990; Sweeney and Burnham, 1990).

5. Discussion

5.1. Characteristics of natural gases in the Kuqa Depression

Natural gas, dominated by a few low-molecular weight gaseous hydrocarbons, is simple compositionally and isotopically. The chemical components and stable carbon isotope compositions of gases from the Kuqa Depression are presented in Table 3, following the early work by Li et al. (2001), Zhao et al. (2002), Liang et al. (2003), Ma et al. (2003), Li et al. (2004), among others. Although the gases appear to have been generated dominantly from the Jurassic coal-bearing sequence, the partial reversal in the stable carbon isotopes of the heavier gaseous alkanes (Table 3) also suggests potential mixing of these gases with those derived from the Triassic sequence (Liang et al., 2003).

For the natural gases discovered in the Kuqa Depression, methane is far more abundant than ethane; the $\delta^{13}C$ values of ethane are much higher than

Table 3
The chemical and stable carbon isotope compositions of natural gases in the Kuqa Depression

SS* Belt	Well/field	Depth(m) or pay zone	Carbon isotope composition (‰)				Components (%)	
			δC_1	δC_2	δC_3	δC_4	Methane	Ethane
Kelasu	KL2	3499.87–3534.66	−27.30	−19.40	−18.50	−17.80	98.05	0.40
	KL2	3803–3809	−27.80	−18.70	/	/	98.03	0.42
	KL2	3888–3895	−27.80	−19.00	−19.10	−20.44	98.22	0.53
	KL3	E	−27.95	−18.25	−17.10	/	96.39	0.62
	KL3	3104.58–3198.79	−25.10	−18.80	/	/	98.05	0.62
	KL201	3630–3640	−27.07	−18.48	−19.08	−20.31	97.86	0.36
	KL201	3770–3795	−27.19	−17.87	−19.14	−20.55	98.87	0.69
	KL201	3936–3938	−26.16	−18.09	−19.06	−22.14	97.08	0.05
	KL202	1472–1481	−28.24	−18.86	−19.15	−20.91	/	/
	DB1	5568.08–5620	−29.33	−21.39	−20.80	−21.91	91.44	∼2.17
	DB2	5658–5669.5	−30.80	−21.50	−19.80	/	96.11	2.18
	DWQ	N_2–K	−32.59	−21.41	−23.21	−23.71	88.59	∼4.26
Yiqikelik	TZ1	1680–1684	−29.38	−18.63	−18.34	−19.63	90.41	5.11
	TZ2	1804–1813	−31.20	−19.80	−18.50	/	94.23	3.75
	TZ2	1886–1896	−31.50	−17.80	−24.30	/	94.65	3.49
	TZ3	1628.5–1697.5	−31.50	−18.70	−20.10	/	95.03	3.07
	TZ3	1839–1842	−31.90	−20.90	−25.50	/	94.34	3.28
	YN2	4776–4785	−32.20	−24.55	−23.07	−22.78	90.86	5.02
	YN2C	4606–4620	−35.99	−27.56	−24.35	−23.61	/	/
	YN4	3619.39–3677.1	−30.67	−25.76	−24.40	−25.40	/	/
	YX1	1908–1925	−35.50	−23.40	−20.60	−21.60	/	/
	YX1	2340–2367	−38.40	−24.20	−21.90	−19.30	/	/
Qulitag	DN2	N	−36.90	−21.30	−24.40	−24.70	88.68	7.24
	DN2	4597–4876	−34.30	−20.90	−15.60	−25.90	/	/
	DN201	4980–4990	−35.2	−23.1	−19.7	−21.2	/	/
	DN202	5022–5046	−35.5	−23.0	−20.8	−24.6	/	/
	DN202	5192–5280	−34.4	−22.6	−20.1	/	/	/
Front Uplift	YH1	E	−34.92	−21.58	−20.33	−23.08	84.18	∼5.67
	TIG	K, N_1	−35.47	−23.50	−21.33	−21.94	80.20	∼7.85
	TB	K	−37.37	−23.33	−25.00	−23.67	82.34	∼7.02
	YH2	K	−38.68	−23.47	−22.09	−23.50	83.97	∼5.46
	YH3	4980–4983	−38.74	−24.69	−22.26	−22.28	88.15	2.98
	YH6	5160–5163	−36.75	−23.88	−22.58	−21.80	/	/
	YD2	K	−37.50	−21.50	−24.50	−23.70	82.88	∼6.85
	YTK	E, K	−38.56	−23.74	−24.01	−24.40	85.97	∼5.21
	Tai2	E, K	−37.43	−22.10	−20.97	−21.20	72.00	∼8.62
	DQ5	/	−38.80	−21.30	−18.6	/	/	/
	YT101	/	−36.20	−23.20	−20.90	/	/	/
	YM7	E	−33.76	−22.88	−22.34	−23.98	84.64	∼4.75

SS* = substructure; /: no data; ∼: the values estimated after C_{2+}.

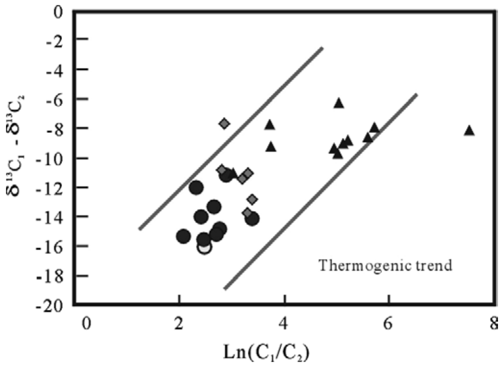

Fig. 3. The $\delta^{13}C_1$–$\delta^{13}C_2$ versus $\ln(C_1/C_2)$ plot showing thermogenic origin of the gases from the Kuqa Depression.

those of methane. These gases are clearly thermogenic, as indicated by the plot of δC_1–δC_2 versus ln(C1/C2) (Fig. 3), originally proposed by Prinzhofer and Huc (1995).

Laterally, the chemical and isotopic compositions of the discovered gases vary systematically across the Kuqa Depression. Compositionally, drier gases are in the Kelasu, wetter gases in the Yiqikelik, and more condensates in the Front Uplift. Higher $\delta^{13}C$ values of the hydrocarbon gases tend to occur in gases from the Front Uplift than those from the Kelasu and Yiqikelik belts. Earlier work by Liang et al. (2002) demonstrated that the hydrocarbon seepage near the northern boundary fault zones of this depression originated from the Triassic source rocks.

5.2. Natural gases generation and expulsion

Chemical adsorption is considered as an important control on the expulsion of oil from coals. A general expulsion threshold value (100 mg oil/g TOC for oil and 20 mg gas/g TOC for gas) has been proposed for oil and gas expulsion from coals (Pepper and Corvi, 1995).

The maximum yield of C_{15+} hydrocarbons (40.65 mg HC/g TOC) measured in our pyrolysis experiment is much lower than the threshold value for oil expulsion proposed by Pepper and Corvi (1995). The absorption of generated petroleum within solid organic matter in source rock is significant, thus selective absorption is likely responsible for the observed compositional differences between migrated petroleum and bitumen extracted from source rocks (Sandvik et al., 1994). Obviously, the C_{15+} hydrocarbons were retained in the coal and subjected to secondary cracking during subsequent maturation. Light hydrocarbons form only at maturities higher than 1.0 %Ro when cracking becomes more dominant. Expulsion begins relatively late. The expelled petroleum consists of C_1 to C_5 hydrocarbons and heavy aromatics (Ritter and Grover, 2005).

Coals can sorb enough methane to be considered as commercial gas reservoirs. Ethane to butane are sorbed even more strongly than methane (Pepper and Corvi, 1995). The sorption capability of coals is related to the temperature and pressure in the subsurface. In this paper, the gas transformation ratio of 20% (or 1.0 %Ro) is used as the threshold value of gas expulsion and 10% (or 0.8 %Ro) as gas generation onset.

Based on the reconstructed thermal history of the major gas kitchens in the Kuqa Depression (Wang et al., 1999, 2000; Liang et al., 2003), the total gas generation yields were calculated using the kinetics parameters stated above. The generation and expulsion of natural gas is illustrated in Fig. 4 (left), where gas generation and expulsion began at about 29 Ma and 12 Ma, corresponding to vitrinite reflectance values of 0.8 and 1.0 %Ro, respectively. As the early-generated gas (<1.0 %Ro) was not expelled out of the coal because of adsorption on the coal matrix, the chemical and isotopic compositions of the early-generated gases are largely inaccessible in natural samples.

The structural evolution scheme shown in Fig. 4 (right) suggests that the effective traps in the study area formed during 5.3–2 Ma, and the thrust faults ultimately cut through the Jurassic and Triassic coal-bearing strata to the bottom of the Tertiary seal, thus providing an effective pathway for natural gas migration. Therefore, gaseous hydrocarbons (C_{2+}) originally trapped in the deep sandstone reservoirs could have experienced thermal cracking under elevated temperatures.

5.3. Origin of natural gases in the Kuqa Depression

The chemical and stable carbon isotopic compositions of natural gases can be used to infer the origin, generation process and post-genetic variance of natural gases. The kinetics of the total gas transformation ratio were modeled at two different heating rates (2 and 10 °C/Ma). The transformation ratio was coupled to Easy%Ro at different heating rates. The results indicate that the transformation ratio of total gas is independent of heating history (Fig. 5a), which is in agreement with the results of Waples and

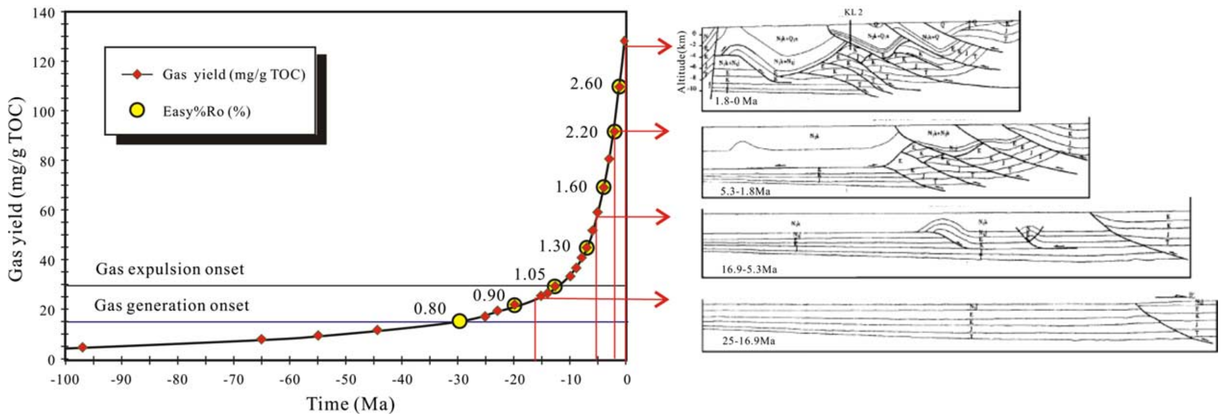

Fig. 4. Structural evolution, source rock maturation and gaseous hydrocarbon generation/expulsion suggested by kinetics modeling. The Jurassic source rocks at the center of Baicheng sag reached approximately 1.0 %Ro and gas expulsion threshold at about 12 Ma. Structural evolution model (Liu et al., 2001) indicates a time of effective trap formation at about 5.3–2 Ma.

Marzi (1998). Waples and Marzi (1998) demonstrated that the correlation between the vitrinite reflectance calculated (i.e., Easy%Ro) and hydrocarbon transformation ratio is not affected by the rock's thermal history to any significant degree for a given kerogen.

Furthermore, the modeling of carbon isotope kinetics for methane and ethane was performed at heating rates of 2 and 10 °C/Ma. As shown in Fig. 5b and c, the stable carbon isotope compositions of both methane and ethane are also independent of thermal histories, unlike vitrinite reflectance. The dependence of the conversion and carbon isotope compositions on the thermal histories is possibly hidden in Easy%Ro, which is strongly related to thermal histories. As Waples and Marzi (1998) pointed out, the specific correlation between %Ro and TR (conversion) is highly dependent of the nature of kerogen. A given kerogen has its kinetic parameters for generation and isotope variance of gaseous hydrocarbons. This specific correlation suggests that it can be used to distinguish the origin of gases within a wide maturity range and heating rates, once this relationship is established. Faber and Stahl (1984) and Tang (2004) gave some cases of coupling of methane-ethane isotope ratios and vitrinite reflectance.

An integrated plot is necessary to better understand the origin of natural gas and possible post-genetic processes in a basin scale or such a big area as Kuqa Depression. The gas expulsion threshold, vitrinite reflectance and carbon isotope values of the gases are shown in Fig. 6. When the carbon isotope data presented in Table 3 are overlaid, that the following points can be made:

(1) Most of the gases occurring in the Front Uplift area are grouped near the gas expulsion onset, indicating that the gases are not from the Jurassic coal. As shown in Fig. 4, the gases in the Kuqa Depression are mainly thermogenic. Therefore, an acceptable explanation is that the gases are mainly generated from the Triassic source rocks.
(2) All gases in the Kelasu belt are close to the line of carbon isotope and Easy%Ro for the Jurassic coal, suggesting their origin is highly related to that source.
(3) The carbon isotope values of the gases collected from the Yiqikelik belt are highly scattered. Some are near the line; others are far from this line, indicating that these gases are possibly generated from different source rocks and underwent the mixing process. At least some of them were generated from the Triassic strata.
(4) The carbon isotope values of the gases from the Qilitag belt are distributed between the gas expulsion threshold and the fitting line, mixing partly with those of Front Uplift. It indicates that the Triassic source rocks have made an important contribution to these gas pools.

On the diagram of C_2/C_1 versus $\delta^{13}C_1$ (Prinzhofer and Pernaton, 1997; Prinzhofer et al., 2000), two directional trends are shown (Fig. 7). One

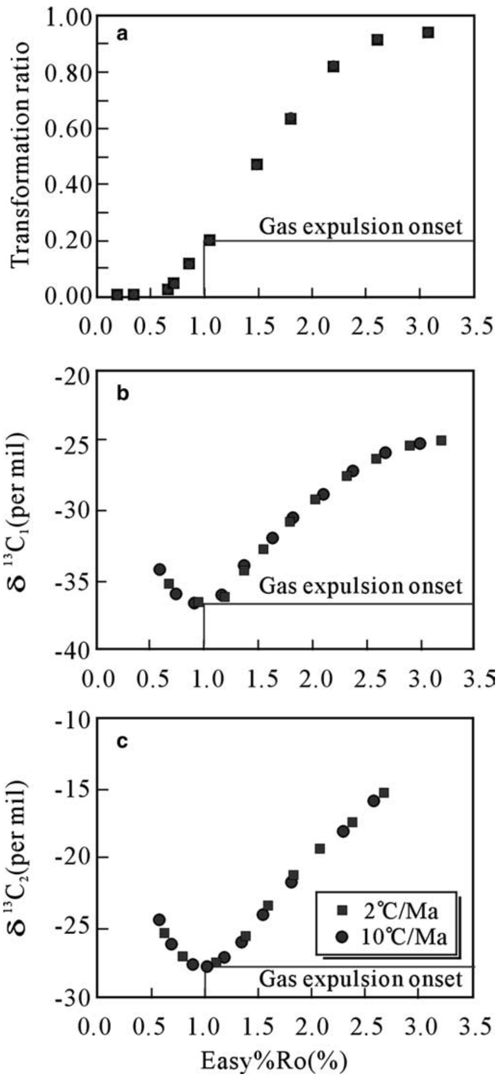

Fig. 5. The modeled relationships between the gas conversion (a), methane isotopic compositions (b), ethane isotopic compositions (c) and Easy%Ro at heating rates of 2 and 10 °C/Ma, respectively. Fig. 6. An integrated plot with C_1–C_2 isotope, Easy%Ro and gas expulsion onset for major source rocks in the Kuqa Depression.

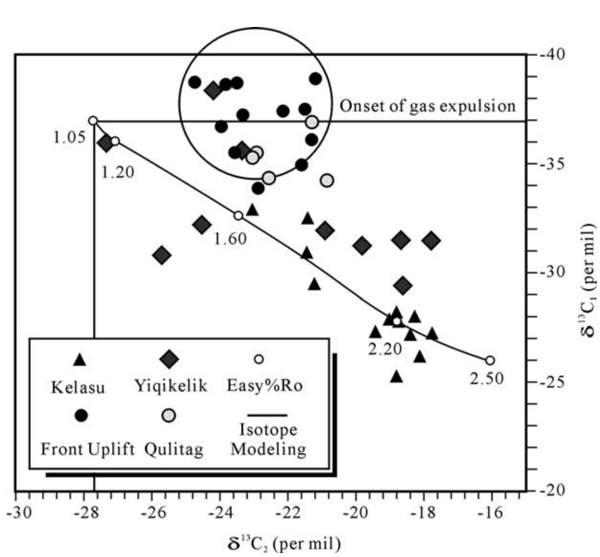

Fig. 6. The integrated plot with C_1–C_2 isotope, Easy%Ro and gas expulsion onset. Two group gases are shown, distinguishing from their origins, thermal histories and accumulation.

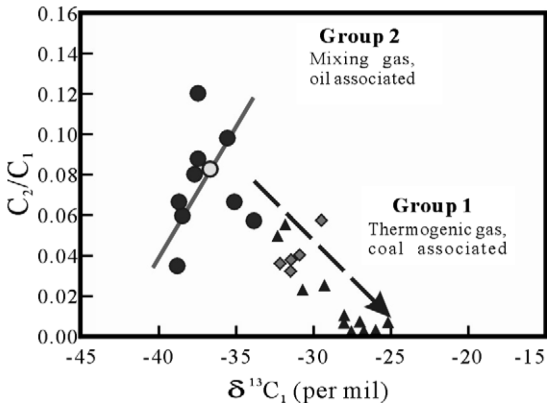

Fig. 7. The C_2/C_1–δC_1 plot showing two directional trends with increasing source thermal maturity. The dicreasing trend in the C_2/C_1 ratio with maturity is related to coal-derived gas, consistent with the model proposed by Prinzhofer and Huc (1995). The trend of increasing C_2/C_1 ratio with maturity is associated with oil generation with mixing from biogenic gas.

shows a decrease of C_2/C_1 ratio with $\delta^{13}C_1$ value, the other exhibits an increase of C_2/C_1 ratio with $\delta^{13}C_1$ value. The former is characterized by dry gas (see also Table 3) and high $\delta^{13}C$ values, indicating a coaly source for the gases. The latter directional trend shows an increase in wet gas content and low $\delta^{13}C$ values, indicating the gases are associated with oil formation. As Prinzhofer and Pernaton (1997) demonstrated, these two directions represent the trends related to maturity and mixing of thermogenic and biogenic gas, respectively. Although the presence of biogenic gas in the Kuqa Depression has yet to be substantiated, data presented in Fig. 7 do suggest that the wet gases with relatively low $\delta^{13}C$ values were not from coal, but rather are gases associated with oil-prone source rocks and mixed with biogenic gas.

As for the two largest gas discoveries in the Kuqa Depression, KL2 field is located in the Kelasu belt, which contains dry gas with relatively high $\delta^{13}C$ values of methane and ethane. These gases are typical of the gases generated from the Jurassic coal measures in the Baicheng sag. The gas source rocks reached the gas expulsion threshold at around 12 Ma (Miocene), and have reached a maturity level of up to 2.2 %Ro. In contrast, the DN2 field of the Qulitag belt contains wet gas with relatively low $\delta^{13}C$ values of methane and ethane. These gases are geochemically similar to those of the Front Uplift gases (Figs. 3, 6, and 7), indicating a Type II–III source, perhaps in the Triassic strata.

6. Conclusions

The kinetic modeling of gas generation using both methane and ethane stable carbon isotope compositions from the Kuqa Depression of the Tarim Basin, NW China demonstrates that the $\delta^{13}C_1$–$\delta^{13}C_2$ cross plot, once integrated with the gas expulsion onset and vitrinite reflectance, is very helpful for assessing the origin and post-genetic changes of natural gases in a large area, even on basinal scale. The gases in the Kuqa Depression are mainly thermogenic. The two maturity trends recognized on the C_2/C_1–$\delta^{13}C_1$ plot indicate that one group of the gases is related to Jurassic coal measures, while another to Triassic lacustrine source rocks with some biogenic gas contribution. These two groups of gases are distributed along different structural belts in the Kuqa Depression, with typical examples in the Kela 2 and Dina 2 fields.

Acknowledgements

We thank Drs. J.Z. Liu and W.L. Jia for their assistance in carrying out pyrolysis experiments and isotopic analysis. This work was supported financially by the China National Key Foundation Project (Grant: 2001CB209101) and the Natural Sciences Foundation of China (Grant Nos. 40272067; 40572083 and 40072053). Prof. L.R. Snowdon is gratefully acknowledged for his comments and language improvements. Dr. Maowen Li (Geological Survey of Canada), Mr. Jim Preston and an anonymous reviewer are thanked for constructive comments on the manuscript.

Associate Editor—**Maowen Li**

References

Behar, F., Kressmann, S., Rudkiewicz, J.L., 1992. Experimental simulation in a confined system and kinetics modelling of kerogen and oil cracking. Organic Geochemistry 19 (1–3), 173–189.

Burnham, A.K., Braun, R.L., 1999. Global kinetic analysis of complex materials. Energy & Fuels 13 (1), 1–22.

Clayton, C., 1991. Carbon isotope fractionation during natural gas generation from kerogen. Marine and Petroleum Geology 8 (2), 232–240.

Cramer, B., Krooss, B.M., Littke, R., 1998. Modeling isotope fractionation during primary cracking of natural gas: a reaction kinetic approach. Chemical Geology 149 (3/4), 235–250.

Cramer, B., Faber, E., Gerling, P., Krooss, B.M., 2001. Reaction kinetics of stable carbon isotopes in natural gas-insights from dry, open system pyrolysis experiments. Energy & Fuels 15 (3), 517–532.

Durand, B., Nicais, G., 1980. Procedure for kerogen isolation. In: Durand, B. (Ed.), Kerogen: Isolated Organic Matter from Sedimentary Rocks. Editions Technip, Paris, pp. 35–52.

Faber, E., Stahl, W., 1984. Geochemical surface exploration for hydrocarbons in the North Sea. American Association Petroleum Geologists Bulletin 68 (3), 363–386.

Galimov, E.M., 1988. Sources and mechanisms of formation of gaseous hydrocarbons in sedimentary rocks. Chemical Geology 71 (1/4), 77–96.

Li, J., Xie, Z., Li, Z., Luo, X., Hu, G., Gong, S., 2001. A gas source study for Kuqa depression of Tarim Basin. Petroleum Exploration and Development 28 (5), 29–41 (in Chinese, English abstract).

Li, M., Bao, J., Wang, H., Zhang, Q.-C., Zheng, D.-M., Lu, Y.-H., Huang, L.-C., 2004. The analysis on the maturity parameters of source rock and hydrocarbon in Kuche foreland basin of Tarim Basin. Natural Gas Geosciences 15 (4), 367–378 (in Chinese, English abstract).

Li, Z., Wang, Q., Wang, D., Lin, W., 2003. Positional record constraints on Late Cenozoic uplift of Tian Shan and tectonic transformation in Kuqa depression, West China. Acta Sedimentologica Sinica 21 (1), 38–45 (in Chinese, English abstract).

Liang, D., Zhang, S., Zao, M., Wang, F., 2002. The petroleum pool of Kuqua depression. Chinese Sciences Bulletin 47 (Suppl.), 56–63 (in Chinese).

Liang, D., Zhang, S., Chen, J., Wang, F., Wang, P., 2003. Organic geochemistry of oil and gas in the Kuqa depression, Tarim Basin, NW China. Organic Geochemistry 34, 873–888.

Lin, C., Liu, J., Zhang, Y., Xiao, J., Chen, J., Ji, Y., 2002. Depositional architecture of the Tertiary tectonic sequences and their response to foreland tectonism in the Kuqa depression, the Tarim Basin. Science in China (D) 45 (3), 250–258.

Liu, H., Qin, T., Yang, Z., 2003a. Sedimentary facies of the Triassic-Jurassic strata in the Tarim Basin, Xinjiang. Sedimentary Geology and Tethyan Geology 23 (1), 37–44 (in Chinese, English abstract).

Liu, W., Song, Y., Liu, Q., Qin, S., Wang, X., 2003b. Evolution of carbon isotope composition in pyrolytic gases generated from coal and its main macerals. Acta Sedimentologica Sinica 21 (1), 183–190 (in Chinese, English abstract).

Liu, Z., Lu, H., Jia, C., 2001. Structures and hydrocarbon accumulation in Kuqa rejuvenated foreland basin. Oil and Gas Geology 22 (4), 297–303 (in Chinese, English abstract).

Lorent, F., Prinzhofer, A., Behar, F., Huc, A.-Y., 1998. Carbon isotope and molecular constrains on the formation and the expulsion of thermogenic hydrocarbon gases. Chemical Geology 147 (3–4), 249–264.

Ma, Y., Xie, H., Cai, Z., Zhang, L., Gao, G., 2003. The geology feature of Dina 2 gas field, Kuche depression. Natural Gas Geosciences 14 (5), 371–374 (in Chinese, English abstract).

Mattavelli, L., Ricchiuto, T., Grignani, D., Cahoell, M., 1983. Geochemistry and habitat of natural gases in Po basin, Northern Italy. American Association of Petroleum Geologists Bulletin 67 (12), 2239–2254.

Pepper, A.S., Corvi, P.J., 1995. Simple kinetic models of petroleum formation. Part III: modelling an open system. Marine and Petroleum Geology 12, 417–452.

Pi, X., Xie, H., Zhang, C., Tian, Z., Zou, H., 2002. Abnormal pressure formation mechanism in Kuqa foreland thrust belt and its effect on gas pool formation. Chinese Science Bulletin 47 (Suppl.), 84–90 (in Chinese).

Prinzhofer, A., Huc, A.Y., 1995. Genetic and post-genetic molecular and isotopic fractionations in natural gases. Chemical Geology 126 (3–4), 281–290.

Prinzhofer, A., Pernaton, E., 1997. Isotopically light methane in natural gases: bacterial imprint or fractionation? Chemical Geology 142, 193–200.

Prinzhofer, A., Vegab, M.A.G., Battanic, A., Escudero, M., 2000. Gas geochemistry of the Macuspana Basin (Mexico): thermogenic accumulations in sediments impregnated by bacterial gas. Marine and Petroleum Geology 17, 1029–1040.

Ritter, U., Grover, A., 2005. Adsorption of petroleum compounds in vitrinite: implications for petroleum expulsion from coal. International Journal of Coal Geology 62, 183–191.

Sandvik, E.I., Young, W.A., Curry, D.J., 1994. Expulsion from hydrocarbon sources: the role of organic absorption. Organic Geochemistry 19 (1–3), 77–87.

Schaefer, R.G., Schenk, H.J., Hardelauf, H., Harms, R., 1990. Determination of gross kinetic parameters for petroleum formation from Jurassic source rocks of different maturity levels by means of laboratory experiments. Organic Geochemistry 16 (1–3), 115–120.

Schaefer, R.G., Galushkin, Y.I., Kolloff, A., Littke, R., 1999. Reaction kinetics of gas generation in selected source rocks of the West Siberian Basin: implications for the mass balance of early-thermogenic methane. Chemical Geology 156 (1–4), 41–65.

Schoell, M., 1980. The hydrogen and carbon isotopic composition of methane from natural gases of various origins. Geochimica et Cosmochimica Acta 44 (5), 649–661.

Schoell, M., 1983. Genetic characterization of natural gases. American Association of Petroleum Geologists Bulletin 67 (12), 2225–2238.

Song, Y., Xia, X., Hong, F., Qin, S., Fu, G., 2002. Characters of abnormal pressure and gas pool patterns of foreland basin. Chinese Science Bulletin 47 (Suppl.), 70–76 (in Chinese).

Stahl, W., 1977. Carbon and nitrogen isotopes in hydrocarbon research and exploration. Chemical Geology 20 (2), 121–149.

Stahl, W., Carey, B.D., 1975. Source-rock identification by isotope analyses of natural gases from fields in the Val Verde and Delaware basins, West Texas. Chemical Geology 16 (4), 257–267.

Sweeney, J.J., 1990. BASMAT Fortran program calculates oil and gas generation using a distribution of discrete activation energies. Geobyte 5 (1), 37–43.

Sweeney, J.J., Burnham, A.K., 1990. Evaluation of a simple model of vitrinite reflectance based on chemical kinetics. American Association of Petroleum Geologists Bulletin 74 (10), 1559–1570.

Tang, Y., 2004. Available from: <http://geoisochem.com/casesstudies.htm>.

Tang, Y., Perry, J.K., Jenden, P.D., Schoell, M., 2000. Mathematical modelling of stable carbon isotope ratios in natural gases. Geochimica et Cosmochimica Acta 64 (5), 2673–2687.

Ungerer, P., Pelet, R., 1987. Extrapolation of oil and gas formation kinetics from laboratory experiments to sedimentary basins. Nature 327 (6117), 52–54.

Wang, F., Zhang, S., Zhang, B., Zhao, M., 1999. Organic maturity of Mesozoic source rocks in Kuqa depression, Tarim Basin, Xinjiang. Petroleum Geology 20 (3), 221–224 (in Chinese, English abstract).

Wang, F., You, M., Liu, C., Zhang, S.C., Zhang, B., Zhao, M., Qin, S., Zhao, J., 2000. Thermal maturation and hydrocarbon generation history of the Mesozoic source rocks in the Kuqa foreland region of the Tarim Basin. In: Abstracts of the 8th Chinese National Meeting on Organic Geochemistry. China Petroleum Society, Beijing, pp. 55–57 (in Chinese).

Waples, D.W., Marzi, R.W., 1998. The universality of the relationship between vitrinite reflectance and transformation ratio. Organic Geochemistry 28 (6), 383–388.

Zhang, H., Shou, J., Chen, Z., Wang, S., Yang, X., Pi, X., Cai, Z., 2002a. Sedimentary characteristics and sandstone body distribution of the Lower Jurassic in Kuqa depression. Journal of Palaeogeography 14 (13), 47–58 (in Chinese, English abstract).

Zhang, J., Chen, J., Zhang, C., Wang, P., 2002b. Relationships between biomarker composition and maturity in coal of Kuche Depression. Journal of Jianghan Petroleum Institute 24 (12), 27–29 (in Chinese, English abstract).

Zhao, M.J., Lu, S.F., Wang, T.D., Li, J., 2002. Geochemical characterization and pool formation processes of natural gases in Kela 2 Gas Field. Chinese Sciences Bulletin 47 (Suppl.), 109–115 (in Chinese).

Zou, Y.-R., Wang, L.Y., Shuai, Y.H., Peng, P.A., 2005. EasyDelta: a spreadsheet for kinetic modeling of the stable carbon isotope composition of natural gases. Computers & Geosciences 31 (7), 811–819.